

Department of Meteorology, University of Utah, Salt Lake City, Utah, U.S.A.

Exploration of the Remote Sounding of Infrared Cooling Rates Due to Water Vapor

Kuo-Nan Liou and Yongkang Xue

With 3 Figures

Received July 7, 1987

Revised September 4, 1987

Summary

We explore the feasibility of deriving atmospheric infrared cooling rates by direct inversion of radiances observed by satellites from space. In order to convert radiances to fluxes and achieve vertical profiling at the same time, we show that it is necessary to combine radiances from narrow channels with radiances averaged over spectral bands. We demonstrate that the vertical integral of the cooling rate in the spectral band, convolved with a kernel function associated with the narrow channel, can be related to a weighted sum of the channel and band radiances. The band radiance must be evaluated at a specific zenith angle, which is a result of use of the mean value theorem. With known kernel functions, the combined radiances may be inverted to obtain the cooling rate profile. These results are derived from use of a random model for the transmittance in its strong- and weak-line limits. The results are similar in the two limits leading us to conclude that there are expressions that are approximately valid over the entire range of transmittance. We show by numerical methods that this conclusion is correct and apply the retrieval technique successfully to get the cooling rate profile in the rotational band of water vapor.

1. Introduction

While significant advances have been made in the determination of temperature and moisture fields from satellites, a direct approach to derive atmospheric infrared cooling rates from space has not been attempted. Two issues are involved. The first issue is whether the cooling rate profile, which is a result of infrared flux divergences within the atmosphere, can be related to emergent radiances

at the top of the atmosphere. The second issue is whether it is possible to find appropriate weighting functions for the performance of retrievals. In this paper, we wish to explore the fundamental principles for deriving infrared cooling rates by direct inversion of satellite radiances.

A direct measurement of infrared cooling rates could have important advantages. Radiation algorithms for cooling rate calculations can use very large amounts of computer time and the differences between different algorithms, even with the same input data, are notorious. A direct relationship between the input data from satellites and the diabatic heating terms required for numerical weather prediction could reduce these uncertainties and save time and effort at the same time. In addition, information on the infrared cooling rate profile can be used to obtain vertical velocities. A simple direct method could be of value to researchers who might wish to have this information.

The history of infrared soundings from satellites is one of slow evolution of retrieval techniques. To be successful, the ideas presented here will require refinement and many additional aspects of the technique will have to be looked into eventually. The prime objective of this paper, then, is to present the general principles involved in retrieval of the infrared cooling rate profile. In Section 2 we shall demonstrate the retrieval tech-

nique using a random model of transmittance with pressure scaling and in the strong- and weak-line limits. This enables us to relate a convolution of the cooling rate in the spectral retrieval band, using an appropriate kernel function for a narrow channel, to a linear combination of band and channel radiances. There are slight differences between the results for the strong- and weak-line limits but they are close enough to be combined empirically in an expression that is valid over the entire range of transmittances. This is done in Section 3, where we also demonstrate the retrieval technique for two broadbands in the water vapor rotational region.

2. Principles of Remote Sensing of Infrared Cooling Rates

There is no obvious relationship between atmospheric cooling rates and emergent radiances at the top of the atmosphere. To the extent that both are associated with temperature and specific gaseous profiles, it seems reasonable to assume that there may be a direct link between the two. Our approach is to introduce a kernel function and to investigate the result of a convolution with the infrared cooling rate profile. The cooling rate, $\dot{\theta}$, expressed in the height coordinate, is related to the net flux divergence by

$$\dot{\theta} = -\frac{1}{\rho_a C_p} \frac{dF(z)}{dz}, \quad (1)$$

where z is the height, C_p the specific heat at constant pressure, ρ_a the density of air, and F the net flux, which is the difference between upward and downward fluxes. In the analyses presented below, the path length coordinate will be used. Radiation quantities without a suffix ($\dot{\theta}$, F , etc.) refer to the spectral retrieval band. In contrast, a suffix i is used to indicate radiation quantities for the kernel channel (spectral sub-band).

We introduce a kernel function in the form

$$K_i(z) = C_p \rho_a(z) T_i[\eta(z)], \quad (2)$$

where T_i denotes the transmittance for an absorber path length, $\eta(z)$ above the level z . We shall include pressure effects by means of pressure scaling so that η is the only independent variable. We then examine the convolution

$$f_i = \int_0^{\infty} \dot{\theta}(z) K_i(z) dz = - \int_0^{\infty} T_i[\eta(z)] \frac{dF(z)}{dz} dz. \quad (3)$$

The idea here is to develop an integral equation containing the infrared cooling rate profile, which is weighted by a kernel function. This kernel function has similarities to those used for temperature soundings. The next step is to correlate the last expression in Eq. 3 to emergent radiances at the top of the atmosphere. By changing variables in Eq. 3, we write

$$f_i = \int_0^{\eta_1} T_i(\eta) \frac{dF(\eta)}{d\eta} d\eta, \quad (4)$$

where η_1 is the pressure corrected path length in the entire atmosphere.

To carry out the integration, expressions for the upward and downward fluxes are required. They are

$$\begin{aligned} F^\uparrow(\eta) &= 2\pi B(\eta_1) \int_0^1 T[(\eta_1 - \eta)/\mu] \mu d\mu \\ &\quad + 2\pi \int_0^1 \int_{\eta_1}^{\eta} B(\eta') \\ &\quad \cdot \frac{dT[(\eta' - \eta)/\mu]}{d\eta'} d\eta' \mu d\mu, \end{aligned} \quad (5a)$$

$$F^\downarrow(\eta) = 2\pi \int_0^1 \int_0^{\eta} B(\eta') \frac{dT[(\eta - \eta')/\mu]}{d\eta'} d\eta' \mu d\mu, \quad (5b)$$

where μ is the cosine of the zenith angle and B the Planck function. The net flux divergence is

$$\begin{aligned} \frac{dF}{d\eta} &= \frac{dF^\uparrow}{d\eta} - \frac{dF^\downarrow}{d\eta} \\ &= 2\pi B(\eta_1) \int_0^1 \frac{\partial}{\partial \eta} T[(\eta_1 - \eta)/\mu] \mu d\mu \\ &\quad + 2\pi \int_0^1 \mu d\mu \left\{ \int_{\eta_1}^{\eta} B(\eta') \right. \\ &\quad \cdot \left. \frac{\partial}{\partial \eta} \left(\frac{dT[(\eta' - \eta)/\mu]}{d\eta'} \right) d\eta' \right\} \end{aligned}$$

$$\begin{aligned}
& + B(\eta) \left. \frac{dT[(\eta' - \eta)/\mu]}{d\eta'} \right|_{\eta'=\eta} \Bigg\} \\
& - 2\pi \int_0^1 \mu d\mu \left\{ \int_0^{\eta_1} B(\eta') \frac{\partial}{\partial \eta} \left(\frac{dT[(\eta - \eta')/\mu]}{d\eta'} \right) d\eta' \right. \\
& \left. + B(\eta) \left. \frac{dT[(\eta - \eta')/\mu]}{d\eta'} \right|_{\eta'=\eta} \right\}. \quad (6)
\end{aligned}$$

We now use the random model (Goody, 1952) modified by Möller and Raschke (1964) to include pressure scaling in the form

$$T_i(\eta/\mu) = \exp \left[- \frac{a l_i \eta}{\mu} \left(1 + \frac{b l_i \eta}{\mu} \right)^{-1/2} \right]. \quad (7)$$

In Eq. 7, $\eta = u(P/P_0)^n$ where n is the scaling parameter, u is the path length, P is the pressure, P_0 is a reference pressure, a and b are certain coefficients given by Möller and Raschke (1964), and l_i is the generalized absorption coefficient of Elsasser and Culbertson (1960). For water vapor, Möller and Raschke (1964) used $n = 0.72$. Equation 7 is usually considered to be a good approximation for narrow spectral bands for water vapor. We shall use this equation for both the spectral retrieval band and narrow channels. We do this to demonstrate a relationship that we confirm by numerical methods, without approximations. Use of the random model for either bands or channels is, at this point, only a matter of convenience.

Under the limits of weak- and strong-line approximations, the random model transmittance reduces to an exponential function of a single variable,

$$T_i(\eta/\mu) = \begin{cases} \exp(-a l_i \eta/\mu) & \text{weak line} \\ \exp(-c l_i^* \eta^*/\mu^*) & \text{strong line} \end{cases} \quad (8)$$

where $c = a/\sqrt{b}$, $l_i^* = \sqrt{l}$, $\eta^* = \sqrt{\eta}$, and $\mu^* = \sqrt{\mu}$. In the weak-line limit, Eq. 6 becomes

$$\begin{aligned}
\frac{dF}{d\eta} &= 2\pi (a l)^2 \int_{\eta}^{\eta_1} B(\eta') \\
&\cdot \int_0^1 \exp[-a l(\eta' - \eta)/\mu] \frac{d\mu}{\mu} d\eta'
\end{aligned}$$

$$\begin{aligned}
& + 2\pi (a l)^2 \int_0^{\eta_1} B(\eta') \int_0^1 \exp[-a l(\eta - \eta')/\mu] \frac{d\mu}{\mu} d\eta' \\
& + 2\pi (a l) B(\eta_1) \int_0^1 \exp[-a l(\eta_1 - \eta)/\mu] d\mu \\
& - 4\pi (a l) B(\eta). \quad (9)
\end{aligned}$$

We also substitute the weak-line limit for the channel transmittance in Eq. 4 to get

$$f_{w,i} = \int_0^{\eta_1} \exp(-a l_i \eta) \frac{dF(\eta)}{d\eta} d\eta, \quad (10)$$

where the subscript w denotes the weak-line condition. In this equation, the net flux divergence in η -coordinates is transformed to the l_i space. Since l_i is related to the channel radiance, a connection between the net flux divergence and radiance is then established*. In the Appendix, we show that $f_{w,i}$ is given by

$$\begin{aligned}
f_{w,i} &= I(\bar{\mu}_1) \cdot 2\pi \chi_i [1 + \chi_i \ln(1 - 1/\chi_i)] \\
& + I_i \cdot 2\pi \chi_i \{ \chi_i [\ln(1 + 1/\chi_i) \\
& - \ln(1 - 1/\chi_i)] - 2 \}, \quad (11)
\end{aligned}$$

where the beam-flux approximate parameter

$$\bar{\mu}_1 = [1 + \chi_i \ln(1 - 1/\chi_i)] / \ln(1 - 1/\chi_i), \quad (12)$$

and

$$\chi_i = l/l_i. \quad (13)$$

Equation 11 expresses $f_{w,i}$ as a linear combination of upwelling radiance in the kernel channel I_i and emergent radiance in the spectral retrieval band I . The latter quantity is evaluated at a mean zenith angle of $\cos^{-1} \bar{\mu}_1$ based on the mean value theorem. It is noted from Eq. 12 that $\bar{\mu}_1$ is a function of the kernel channel. The procedure for getting $\bar{\mu}_1$ is similar to but not exactly the same as the relation between slab and column transmittances proposed by Elsasser (1942) and used by many subsequent workers. The logarithmic function in Eqs. 11 and 12, requires that the parameter χ_i must

* If we let $\eta_1 \rightarrow \infty$, Eq. 10 becomes a Laplace transform equation. It is noted that King (1963) originally introduced the Laplace transform technique for remote sounding applications.

be greater than unity, i.e., $l > l_i$. This implies a specific requirement for the selection of channels. It is necessary to choose kernel channels with relatively weaker absorption coefficients than those for spectral retrieval bands. The selection of l and l_i will be discussed in Section 3.

In the strong-line limit, we find from Eqs. 8 and 4

$$f_{s,i} = \int_0^{\infty} \exp(-c l_i^* \eta^*) \frac{dF(\eta^*)}{d\eta^*} d\eta^*, \quad (14)$$

where the s -suffix indicates strong lines. By an analysis similar to that illustrated in the Appendix, we can show

$$f_{s,i} = I(\bar{\mu}_2^*) \cdot 4\pi \chi_i^{1/2} \left[\frac{1}{3} + \frac{1}{2} \chi_i^{1/2} + \chi_i + \chi_i^{3/2} \ln(1 - 1/\chi_i^{1/2}) \right] + I_i \cdot 4\pi \chi_i \left\{ \chi_i [\ln(1 + 1/\chi_i^{1/2}) - \ln(1 - 1/\chi_i^{1/2})] - 2\chi_i^{1/2} - \frac{3}{8} \right\}, \quad (15)$$

where

$$\bar{\mu}_2^* = \frac{\left[\frac{1}{3} + \frac{1}{2} \chi_i^{1/2} + \chi_i + \chi_i^{3/2} \ln(1 - 1/\chi_i^{1/2}) \right]}{\left[\frac{1}{2} + \chi_i^{1/2} + \chi_i \ln(1 - 1/\chi_i^{1/2}) \right]} \quad (16)$$

Finally, to ensure the validity of the solutions derived in Eqs. 11 and 15, computations were carried out for a number of spectral band and channel combinations. Deviations from Eqs. 10 and 14 are less than 0.01%.

In view of the similarities between Eqs. 11 and 15, we postulate that under all conditions

$$f_i = \int_0^{\infty} \hat{\theta}(z) K_i(z) dz = f_1(\chi_i) I(\bar{\mu}) + f_2(\chi_i) I_i, \quad (17)$$

where f_1 , f_2 , and $\bar{\mu}$ are functions similar to those given in Eqs. 11 and 15. Since we could not obtain an analytical solution using the exact random model transmittance, we determine f_1 , f_2 , and $\bar{\mu}$ by numerical methods. This will be discussed in the next section.

We have demonstrated that the information content of the infrared cooling rate profile is related to the upwelling channel and emergent spec-

tral radiances by a Fredholm equation of the first kind. Thus, the idea developed here for remote sounding of cooling rate profiles is a combined utilization of the wavenumber and angular scans. Two fundamental issues are apparent. The first is whether kernel channels can be selected to give satisfactory weights to the cooling rate profile. The next issue is, given I and I_i , whether it is possible to perform retrievals, since the Fredholm equation of the first kind is mathematically ill-conditioned. The latter issue is universal for sounding of atmospheric parameters. The former issue requires a knowledge of the channel transmittances.

3. Physical Analysis and Preliminary Results

3.1 Channel Selection

In this subsection we discuss the selection of channels for the inversion of infrared cooling rates. Figure 1 shows the generalized absorption coefficient as a function of wavenumber for a 600 cm^{-1} interval in the rotational band of water vapor (Möller and Raschke, 1964). Cooling in the troposphere is primarily generated by this band (see, e.g., Liou and Ou, 1981). We use the 40 cm^{-1} channels in Fig. 1 as prospective kernel channels. We may divide the H_2O rotational spectrum into as many retrieval bands as we wish. In practice it

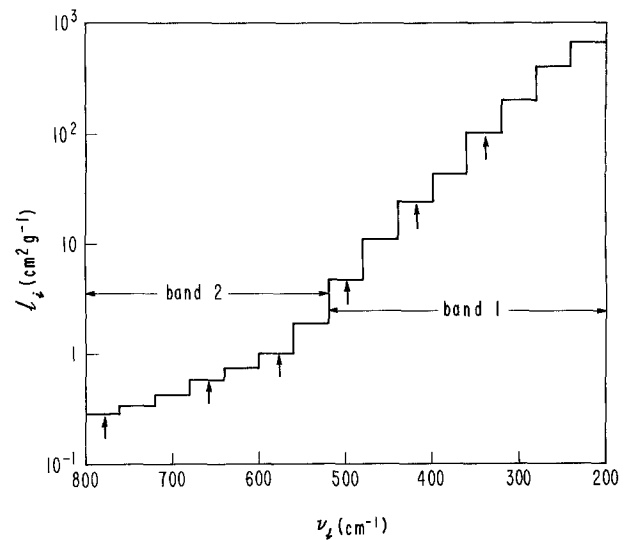


Fig. 1. Generalized absorption coefficient for water vapor as a function of a 40 cm^{-1} interval (after Möller and Raschke, 1964). The channels selected for the inversion of the cooling rate profile are indicated in the diagram by arrows

is desirable to reduce the number of retrieval bands to a minimum. We found by trial and error that two could be used: 200–520 cm^{-1} (band 1) and 520–800 cm^{-1} (band 2). To obtain l_1 and l_2 for these two spectral regions, we average 40 cm^{-1} intervals weighted by the Planck functions at a temperature of 300° K. This choice of $l_{1,2}$ is justified by the results of cooling rate inversions illustrated in subsection 3.3.

The selection of channels is constrained by the requirement $l_{1,2} > l_i$. There are only six wavenumbers indicated by arrows in Fig. 1 that satisfy this restriction and that give weighting functions with sufficient vertical coverage. We have chosen channels centered on 340, 420, 500, and 660 cm^{-1} for band 1 and 580 and 780 cm^{-1} for band 2. Note that there is no reason why the channel should be contained within the retrieval band, provided that all other requirements are satisfied. The normalized weighting functions for the standard atmospheric temperature and water-vapor profiles (McClatchey et al., 1972) are depicted in Fig. 2. Although wavenumbers such as 380 cm^{-1} could also be used in band 1, they add little information to channels 340 and 420 cm^{-1} .

The kernel function introduced in Eq. 3 is the product of the air density and channel transmittance. Since the channel transmittance depends on the water vapor path length, it is appropriate to consider how much this affects the shape of the kernel function. We have employed two additional temperature and water vapor profiles typical of those for midlatitude and subarctic summer conditions (McClatchey et al., 1972) in the computation of the weighting function. We find that the

shapes and peaks of the weighting functions for 420, 580, 660, and 780 cm^{-1} do not vary significantly. These channels have peaks below about 7 km, as shown in Fig. 2. For 340 and 500 cm^{-1} , the peak of the weighting function for a moist midlatitude atmosphere is lowered by about 0.5 km. The reason that the weighting function is fairly stable is, in part, because it involves the air density profile, which is independent of the absorbers.

3.2 Selection of an Adjustment Parameter

Referring to Eq. 17, we need to find analytic forms for f_1 and f_2 . A series of computational experiments were carried out with a number of atmospheric water-vapor and temperature profiles. For the first term we found

$$f_1(\chi_i) = a_i \cdot 2\pi \chi_i [1 + \chi_i \ln(1 - 1/\chi_i)], \quad (18)$$

where for band 1

$$a_i = \begin{cases} (0.972 + 0.143 \chi_i)^{-1}, & 1 < \chi_i < 10 \\ (0.416 + 0.00249 \chi_i), & \chi_i > 10 \end{cases} \quad (19)$$

and for band 2

$$a_i = (1.316 - 0.145 \chi_i)^{-1}. \quad (20)$$

However, the second term is unchanged from that in Eq. 11,

$$f_2(\chi_i) = 2\pi \chi_i \{ \chi_i [\ln(1 + 1/\chi_i) - \ln(1 - 1/\chi_i)] - 2 \}. \quad (21)$$

With these expressions and the expression for $\bar{\mu}$ in Eq. 12, we find that $|f_i - [f_1 I(\bar{\mu}) + f_2 I_i]|$ is less than 0.1% for all channels. The value of $\bar{\mu}$ varies slightly from 0.5 to 0.6 for the channels selected.

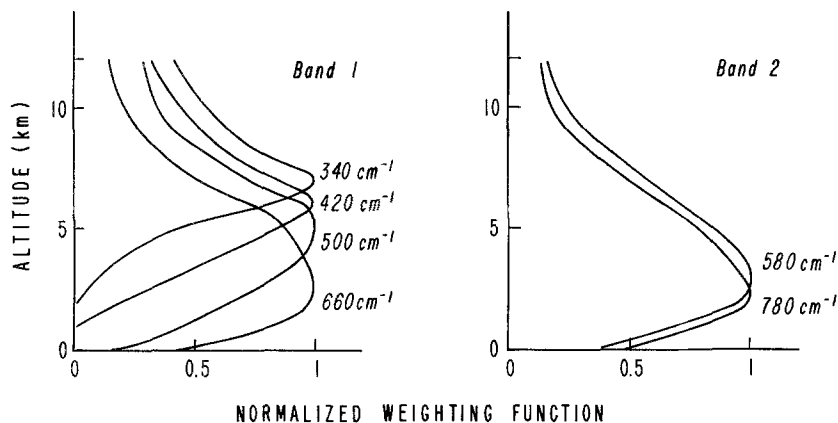


Fig. 2. Normalized weighting functions as a function of altitude for band 1 (200–520 cm^{-1}) and band 2 (520–800 cm^{-1}) in the rotational band of water vapor

3.3 Retrieval Experiments

Cooling rate profiles typically have broad maxima in the middle troposphere. To investigate whether practical retrievals are possible, an exact function is defined in the form

$$g_i = \int_0^{\infty} \dot{\theta}(z) K_i(z) dz. \quad (22)$$

We may also define an error $\varepsilon_i = f_i - g_i$. We seek a solution for $\dot{\theta}$ subject to this error, using the constrained linear inversion method proposed by Phillips (1962) and Twomey (1963). The solution,

in matrix form, is given by

$$\vec{\theta} = (\vec{K}^* \vec{K} + \gamma \vec{H})^{-1} \vec{K}^* \vec{f}, \quad (23)$$

where \vec{K}^* is the transpose of \vec{K} , the kernel function matrix, γ is a Lagrangian multiplier, and \vec{H} is a quadrature constraint for smoothing. The first differences were used to obtain \vec{H} in the retrieval exercises.

Figure 3 (a) and (b) are retrieval results, with and without errors for the standard atmospheric temperature and water vapor profiles. The solid curves are the assumed profiles for the rotational band of water vapor. The dashed lines are sums of cooling rates for bands 1 and 2. Without errors, i.e., using g_i and a smoothing parameter of 0.0005 in the inversion exercises, the retrieved cooling rate profile below about 9 km deviates from the assumed profile by less than $0.2^\circ\text{C}/\text{day}$. Random errors of 2 to 10% were introduced for ε_i in the retrieval shown in Fig. 3 (b). These errors do not degrade the retrieval. In addition to the standard cooling rate profile, two profiles for midlatitude and subarctic summer conditions were employed in the retrieval exercises. The assumed profile for the subarctic summer shows a maximum at about 6 km, which also appears in the retrieval. Between about 8 and 10 km, there were larger deviations. For the midlatitude summer, the cooling rate profile has a well-defined maximum at about 8 km. Although the retrieved maximum is about 1 km lower, the retrieved profile resembles the assumed profile quite closely. These experiments appear to suggest that it should be feasible to invert the infrared cooling profile due to water vapor from satellite radiance measurements.

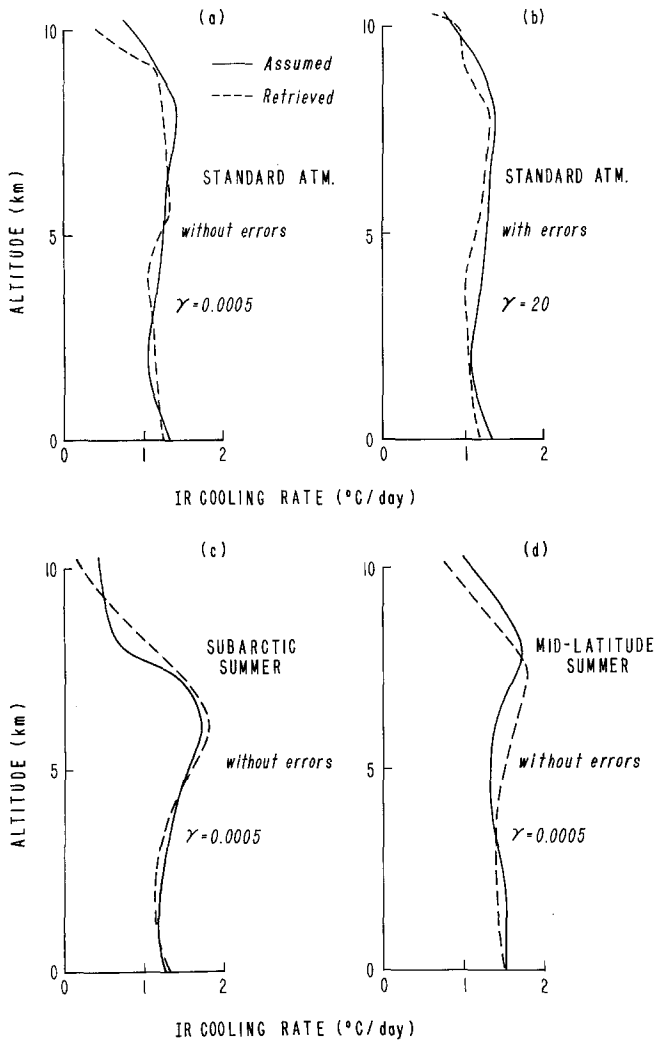


Fig. 3. Retrieved infrared cooling rate profiles for the rotational band of water vapor for the standard atmosphere with (a) and without (b) errors, and for the subarctic summer (c) and midlatitude summer (d) atmospheres without errors. γ is the smoothing parameter

4. Conclusions

We have demonstrated in this paper the theoretical basis and numerical feasibility of inversions leading to the retrieval of atmospheric cooling rates. We showed that the inversion is governed by a Fredholm equation of the first kind, where the kernel function is a product of the channel transmittance and air density. The required measurements from satellites are a set of radiances in the kernel channel and emergent radiances in the spectral retrieval band. The latter quantities must be evaluated at specific zenith angles.

The inversion of the Fredholm equation developed in this paper is stable enough to give sat-

isfactory accuracy for the rotational band of water vapor in specific cases. However, the retrieval equation is ill-posed and must be investigated carefully. We used a linear constraint inversion method that was developed for other inversions and alternative methods may have advantages.

We attempted similar inversions for the 15 μm CO₂ band but failed to find appropriate kernel functions in the stratosphere and lower mesosphere where the CO₂ cooling is significant. The overlap between CO₂ and H₂O bands is a matter that we have not yet considered. This may be a case in which the k -distribution method (Arking and Grossman, 1972) is more illuminating than the use of random model transmittances. The k -distribution technique can give very accurate results for nonhomogeneous absorption paths and can be extended to scattering atmospheres as well. More consideration must be given to the choice of kernel channels and to methods of deriving broad bands for practical retrievals.

The retrieval technique described in this paper would, if adopted, place requirements on the observing system. Measurements must be made at all relevant wavenumbers, which would require a scanning interferometer. In addition, radiances in the spectral retrieval band must be measured at specific zenith angles. This would require an angular scanning device.

Acknowledgements

A part of the research work was carried out while Liou was a visiting scholar at Harvard University. He would like to thank Professor Richard Goody for his hospitality, inspiring discussions, and encouragement. He is also grateful to Professor Goody for numerous exchanges of ideas and critical inquiries into the fundamentals of remote sounding of atmospheric cooling rates, and for his detailed suggestions, which led to a significant improvement in the presentation of the paper. We would also like to thank Dr. Jean F. King for his helpful comments on the paper. Sharon Bennett typed and edited the manuscript. This research was supported in part by the Air Force Geophysics Laboratory under contract F19628-87-K-0042 and NASA Grant NAG5-732.

References

- Arking, A., Grossman, K., 1972: The influence of line shape and band structure on temperatures in planetary atmospheres. *J. Atmos. Sci.*, **29**, 937–949.
- Elsasser, W. M., 1942: Heat transfer by infrared radiation in the atmosphere. Harvard Meteorological Studies, No. 6. Cambridge: Harvard University Press, 107 pp.

- Elsasser, W. M., Culbertson, M. F., 1960: Atmospheric radiation tables. *Meteor. Mongr.*, **4**, 1–43.
- Goody, R. M., 1952: A statistical model for water vapor absorption. *Quart. J. Roy. Meteor. Soc.*, **78**, 165–169.
- King, J. I. F., 1963: Meteorological inferences from satellite radiometry. I. *J. Atmos. Sci.*, **20**, 245–250.
- Liou, K. N., Ou, S. C., 1981: Parameterization of infrared radiative transfer in cloudy atmospheres. *J. Atmos. Sci.*, **38**, 2707–2716.
- McClatchey, R. A., Fenn, R. W., Selby, J. E., Volz, F. E., Garing, J. S., 1972: Optical properties of the atmosphere (3rd ed.). AFCRL-72-0497.
- Möller, F., Raschke, E., 1964: Evaluation of TIROS III radiation data. NASA CR-112, 114 pp. (available from the Office of Technical Services, Department of Commerce, Washington, D.C. 20230).
- Phillips, D. L., 1962: A technique for the numerical solution of certain integral equations of the first kind. *J. Assoc. Comput. Mach.*, **9**, 84–97.
- Thomas, G. B., Jr., Finney, R. L., 1984: *Calculus and Analytic Geometry* (6th edition). Reading, MA: Addison-Wesley, 1041 pp.
- Twomey, S., 1963: On the numerical solution of Fredholm integral equations of the first kind by the inversion of the linear system produced by quadrature. *J. Assoc. Comput. Mach.*, **10**, 97–101.

Authors' address: Prof. Kuo-Nan Liou and Dr. Yongkang Xue, Department of Meteorology, The University of Utah, 819 Wm. C. Browning Bldg., Salt Lake City, UT 84112, U.S.A.

Appendix

Derivation of the Fundamental Equations for Remote Sounding of Infrared Cooling Rates

We begin with Eq. (10)

$$f_{w,i} = \int_0^{\eta_1} \exp[-al_i\eta/\mu] \frac{dF(\eta)}{d\eta} d\eta. \quad (\text{A } 1)$$

Upon substituting the expression for the net flux divergence in Eq. 9 into Eq. A 1, we find

$$\begin{aligned} f_{w,i} = & 2\pi(aI)^2 \int_0^{\eta_1} \exp(-al_i\eta/\mu) \\ & \cdot \left\{ \int_{\eta}^{\eta_1} B(\eta') \left\{ \int_0^1 \exp\left[-\frac{al(\eta' - \eta)/\mu'}{\text{term (a)}} \frac{d\mu'}{\mu'}\right] d\eta'\right\} d\eta \right\} \\ & + 2\pi(aI)^2 \int_0^{\eta_1} \exp(-al_i\eta/\mu) \left\{ \int_0^{\eta} B(\eta') \right. \\ & \cdot \left. \left\{ \int_0^1 \exp\left[-\frac{al(\eta - \eta')/\mu'}{\text{term (b)}} \frac{d\mu'}{\mu'}\right] d\eta'\right\} d\eta \right\} \\ & + 2\pi(aI) B(\eta_1) \int_0^{\eta_1} \left\{ \int_0^1 \exp\left[-\frac{al(\eta_1 - \eta)/\mu'}{\text{term (c)}} \frac{d\mu'}{\mu'}\right] d\mu'\right\} \end{aligned}$$

$$\begin{aligned} & \cdot \exp(-a l_i \eta / \mu) d\eta \\ & - 4\pi(a l) \int_0^{\eta_1} B(\eta) \exp(-a l_i \eta / \mu) d\eta. \end{aligned} \quad (\text{A } 2)$$

We may interchange the order of integrations with respect to η and η' in term (a) to get (see, e.g., Thomas and Finney, 1984, p. 900)

$$\begin{aligned} & \int_0^{\eta_1} B(\eta') \left\{ \int_0^{\eta'} \exp(-a l_i \eta / \mu) \right. \\ & \cdot \left. \int_0^1 \exp[-a l(\eta' - \eta) / \mu'] \frac{d\mu'}{\mu'} \right\} d\eta' . \end{aligned} \quad (\text{A } 3)$$

Let $y = \eta' - \eta$ and rearrange terms, Eq. A 3 becomes

$$\begin{aligned} & \int_0^{\eta_1} B(\eta') \exp(-a l_i \eta' / \mu) \left\{ \int_0^{\eta'} \exp(a l_i y / \mu) \right. \\ & \cdot \left. \int_0^1 \exp(-a l y / \mu') \frac{d\mu'}{\mu'} \right\} d\eta' . \end{aligned} \quad (\text{A } 4)$$

Integration over y leads to

$$\begin{aligned} & \int_0^{\eta_1} B(\eta') \exp(-a l_i \eta' / \mu) \\ & \cdot \left\{ \int_0^1 \left\{ \exp\left[\frac{a(l_i/\mu - l/\mu')\eta'}{\text{term (a 1)}}\right] - 1 \right\} \frac{d\mu'/\mu'}{a(l_i/\mu - l/\mu')} \right\} d\eta' . \end{aligned} \quad (\text{A } 5)$$

With $\chi_i = (l/l_i) \mu$ (note that in the main text we set $\mu = 1$), we may perform the analytic integration for term (a 2) in Eq. A 5. Solutions exist for $\chi \leq 1$ but we shall only consider the case $\chi > 1$,

$$- \int_0^{\eta_1} B(\eta') \exp(-a l_i \eta' / \mu) d\eta' \cdot \left(\frac{\chi_i}{a l} \right) \ln(1 - 1/\chi_i) . \quad (\text{A } 6)$$

For term (a 1) we use the mean value theorem to get

$$\int_0^{\eta_1} B(\eta') \exp(-a l \eta' / \bar{\mu}) d\eta' \cdot \left(\frac{\chi_i}{a l} \right) \ln(1 - 1/\chi_i) . \quad (\text{A } 7)$$

The mean value $\bar{\mu}$ in Eq. A 7 depends on the Planck function profile. Since temperatures in the troposphere and stratosphere of the earth's atmosphere are in the range 200–300 °K, we shall assume an isothermal atmosphere. Thus, for $\eta_1 \rightarrow \infty$, the double integrals in term (a 1) become

$$\begin{aligned} & \int_0^\infty \int_0^1 \exp(-a l \eta' / \mu') \frac{d\mu'/\mu'}{l(1/\chi_i - 1/\mu')} d\eta' \\ & = \int_0^\infty \exp(-a l \eta' / \bar{\mu}) d\eta' \cdot \frac{\chi_i}{l} \ln(1 - 1/\chi_i) \\ & = \frac{\bar{\mu} \chi_i}{a l^2} \ln(1 - 1/\chi_i) . \end{aligned} \quad (\text{A } 8)$$

On the other hand, if we perform the integration with respect to η' first, we obtain

$$\frac{1}{a l^2} \int_0^1 \frac{d\mu'}{(1/\chi_i - 1/\mu')} = \frac{\chi_i}{a l^2} [1 + \chi_i \ln(1 - 1/\chi_i)] . \quad (\text{A } 9)$$

Since we require that the total area under two integrations be equal, we have, from Eqs. A 8 and A 9,

$$\bar{\mu} = [1 + \chi_i \ln(1 - 1/\chi_i)] / \ln(1 - 1/\chi_i) . \quad (\text{A } 10)$$

Using this expression, Eq. A 7 was computed for a number of atmospheric profiles and absorption parameters. The results differ from quantities with variable Planck functions only in the fifth decimal place. This shows that $\bar{\mu}$ is not a strong function of the temperature profile, at least in the earth's atmosphere.

The emergent channel radiance at the top of the atmosphere in the weak-line limit may be expressed by

$$I_i(\mu) = \frac{a l_i}{\mu} \int_0^{\eta_1} B_i(\eta') \exp(-a l_i \eta' / \mu) d\eta' . \quad (\text{A } 11)$$

A similar expression can be written for the spectral radiance. It is noted that the surface contribution may be included in the analysis, but for sounding applications, it suffices to use the atmospheric term. Combining Eqs. A 6 and A 7 and noting that over small spectral regions $B \cong B_i$, term (a) in Eq. A 2 becomes

$$2\pi \chi_i \ln(1 - 1/\chi_i) [\bar{\mu} I(\bar{\mu}) - \chi_i I_i(\mu)] . \quad (\text{A } 12)$$

For term (b) in Eq. A 2, we follow the same procedures. We first interchange the order of integrations to get

$$\begin{aligned} & \int_0^{\eta_1} B(\eta') \left\{ \int_{\eta'}^{\eta_1} \left\{ \exp(-a l_i \eta / \mu) \right. \right. \\ & \cdot \left. \left. \int_0^1 \exp[-a l(\eta - \eta') / \mu'] \frac{d\mu'}{\mu'} \right\} d\eta d\eta' \right\} . \end{aligned} \quad (\text{A } 13)$$

Then we let $y = \eta - \eta'$ and carry out the integration with respect to y , to obtain

$$\begin{aligned} & \int_0^{\eta_1} B(\eta') \exp(-a l_i \eta' / \mu) \left\{ \int_0^1 \left\{ 1 - \exp\left[-\frac{a(l_i/\mu}{\text{term (b 1)}}\right] \right. \right. \\ & \left. \left. + \frac{l_i/\mu'}{\text{term (b 2)}} (\eta_1 - \eta') \right\} \frac{d\mu'/\mu'}{a(l_i/\mu + l/\mu')} \right\} d\eta' . \end{aligned} \quad (\text{A } 14)$$

After integration over η' , term (b 2) in Eq. A 14 will be related to exponential functions involving η_1 . If we let $\eta_1 \rightarrow \infty$, this term approaches zero. This can be done by assuming an isothermal atmosphere. Hence, from Eq. A 11, term (b) in Eq. A 2 becomes

$$2\pi \chi_i^2 \ln(1 + 1/\chi_i) I_i(\mu) . \quad (\text{A } 15)$$

For term (c) in Eq. A 2, integration over η can be performed analytically. The results are exponential functions involving η_1 . Again, if we let $\eta_1 \rightarrow \infty$, this term approaches zero. For finite η_1 , computations show that the contributions of term (b 2) in Eq. A 14 and Eq. A 2 are less than 0.01%. For term (d) in Eq. A 2, we use Eq. A 11 and find

$$-4\pi\chi I_i(\mu). \quad (\text{A } 16)$$

Combining Eqs. A 12, A 15, and A 16, we obtain

$$f_{w,i} = I(\bar{\mu}) \cdot 2\pi\chi_i [1 + \chi_i \ln(1 - 1/\chi_i)] + I_i(\mu) \cdot 2\pi\chi_i \{ \chi_i [\ln(1 + 1/\chi_i) - \ln(1 - 1/\chi_i)] - 2 \}. \quad (\text{A } 17)$$

An analytic solution can be obtained for $f_{s,i}$ in the strong-line limit with the same procedures. In the main text we followed the conventional remote sounding approach by setting $\mu = 1$ so that $\chi_i = l/l_i$. However, it is feasible to measure I_i and I at the same zenith angle, $\cos^{-1} \bar{\mu}_i$, for each kernel channel without affecting our conclusions.